Spatial expression patterns of genes encoding sugar sensors in leaves of C4 and C3 grasses

by Benning, U.F., Chen, L. Watson-Lazowski, A., Henry, C., Furbank, R.T. and Ghannoum, O.

Title Page – Original Article

Spatial expression patterns of genes encoding sugar sensors in leaves of C_4 and C_3 grasses

Short title: Sugar sensor gene expression in C_4 and C_3 grasses

Authors

Urs F. Benning[1†], Lily Chen[1†], Alexander Watson-Lazowski[2], Clemence Henry[1], Robert T. Furbank[3], Oula Ghannoum[1*]

[1]Hawkesbury Institute for the Environment, Western Sydney University, Hawkesbury Campus, New South Wales 2753, Australia

[2]Harper Adams University, Edgmond, TF10 8NB, United Kingdom

[3]ARC Centre of Excellence for Translational Photosynthesis, Research School of Biology, Australian National University, Canberra, Australian Capital Territory 2601, Australia

[†]Equal contribution and co-first authors

[*]Corresponding author: o.ghannoum@westernsydney.edu.au

Background and aims. The mechanisms of sugar sensing in grasses, especially those using C_4 photosynthesis, remains elusive despite being a large proportion of the world's agricultural crops. We addressed this gap by comparing the expression of genes encoding components of sugar sensors in C_3 and C_4 grasses, with a focus on source tissues of C_4 grasses. Given C_4 plants evolved into a two-cell carbon fixation system, it was hypothesised this may have also changed how sugars were sensed.

Methods. For six C_3 and eight C_4 grasses, putative sugar sensor genes were identified for Target of Rapamycin (TOR), SNF1- related kinase 1 (SnRK1), Hexokinase (HXK) and those involved in the metabolism of the sugar sensing metabolite trehalose-6-phosphate (T6P) using publicly available RNA deep sequencing data. For several of these grasses, expression was compared in three ways: source (leaf) vs. sink (seed), along the gradient of the leaf, and bundle sheath vs. mesophyll cells.

Key Results. No positive selection of codons associated with the evolution of C_4 photosynthesis was identified in sugar sensor proteins here. Expression of genes encoding sugar sensors were relatively ubiquitous between source and sink tissues as well as along the leaf gradient of both C_4 and C_3 grasses. Across C_4 grasses, *SnRK1β1* and *TPS1* were preferentially expressed in the mesophyll and bundle sheath cells, respectively. Species specific differences of gene expression between the two cell types were also apparent.

Conclusions. This comprehensive transcriptomic study provides an initial foundation for elucidating sugar sensing genes within major C_4 and C_3 crops. This study provides some evidence that C_4 and C_3 grasses do not differ in how sugars are sensed. While sugar sensor gene expression has a degree of stability along the leaf, there are some contrasts between the mesophyll and bundle sheath cells.

Key words: C_3 and C_4 photosynthesis, hexokinase (HXK), grasses, sink, source, sugar sensing genes, SNF1- related kinase 1 (SnRK1), Target of Rapamycin (TOR), trehalose-6-phosphate (T6P).

Introduction

Given C_4 species fix carbon and synthesise carbohydrates using a two-cell system compared to C_3 species which uses a single cell, it remains unclear if the sugars produced are sensed differently between them. C_4 photosynthesis evolved approximately 35 million years ago in response to a period of low atmospheric CO_2, evolving in 62 independent lineages (Sage 2004, 2017; Sage *et al.* 2011). Many agronomically important cereals, such as *Zea mays* (maize), *Sorghum bicolor* (sorghum), *Panicum virgatum* (switchgrass) and millets (such as *Setaria italica*) utilise C_4 photosynthesis. This evolution has led to major changes in gene expression, leaf morphology, biochemistry and the compartmentalisation of photosynthetic reactions (Dengler and Nelson 1999; Von Caemmerer and Furbank 2003; Mckown and Dengler 2007; Muhaidat *et al.* 2007; Emms *et al.* 2016; Furbank and Kelly 2021).

This compartmentalisation of C_4 photosynthesis is enabled by a specialised leaf anatomy, known as Kranz anatomy, whereby mesophyll cells are arranged in a concentric layer around the bundle sheath cells (Haberlandt 1904; Hattersley 1984). In the mesophyll of C_4 leaves, CO_2 is hydrated into bicarbonate and is initially fixed by phospho*enol*pyruvate (PEP) carboxylase (PEPC), using PEP as a CO_2 acceptor (Hatch and Slack 1966; Furbank and Hatch 1987). Oxaloacetate (OAA) is then produced and rapidly converted to two possible C_4 acids, malate or aspartate. These acids diffuse to the bundle sheath via the abundant plasmodesmatal connections where they are decarboxylated, releasing CO_2 to be refixed by Ribulose-1,5-bisphosphate carboxylase-oxygenase (Rubisco) (Danila *et al.* 2016, 2018). The compartmentalisation of the photosynthetic enzymes, the high PEPC/Rubisco activity ratio and the low permeability of the bundle sheath cell wall elevate CO_2 concentration around Rubisco, leading to near CO_2 saturation and reduced photorespiration (Hatch 1987; Ghannoum *et al.* 2000; Von Caemmerer and Furbank 2003; Danila *et al.* 2021).

During the evolution of C_4 photosynthesis, the expression of numerous genes were adjusted to enable distinct spatial separation, or altered regulation, relative to expression patterns seen in species which utilise C_3 photosynthesis (Hibberd and Covshoff 2010; Westhoff and Gowik 2010; Christin and Osborne 2014). Some examples include the targeted expression of PEPC and the confinement of carbonic anhydrase to the mesophyll cell in C_4 plants as well as differences in Rubisco catalytic efficiencies between the two photosynthetic types (Gowik *et al.* 2004; Tetu *et al.* 2007; Tanz *et al.* 2009; Whitney *et al.* 2011; Ludwig 2016). The evolution of photosynthesis into a two-cell process in C_4 plants has also resulted in the spatial partitioning of carbohydrate production. One of the main products of photosynthesis, triose phosphate, is used in the synthesis of soluble sugars such as glucose and sucrose, substrates which can then be synthesised into the storage carbohydrate starch. Generally, in C_4 plants sucrose biosynthesis occurs in the mesophyll, while starch synthesis occurs predominantly in bundle sheath chloroplasts (Lunn and Furbank 1997, 1999; Lunn 2007; Furbank and Kelly 2021). In leaves of C_3 species these processes occur almost exclusively in the mesophyll. Carbohydrates are moved from the photosynthetic source leaves to the heterotrophic sink tissues such as seeds, stems, roots, and young leaves for growth and development.

Photosynthesis and sink demand are tightly coordinated through metabolic feedback and signalling mechanisms (Blechschmidt-Schneider *et al.* 1989; Sheen 1990). Sugar signalling integrates sugar production with plant development and environmental cues (Rolland *et al.* 2006). To date, there is a limited understanding of the molecular mechanisms underlying those feedback regulations in C_4 plants. C_4 species evolved in arid and warmer climates, conditions that may have also imposed specific selective pressures on aspects of sugar sensing. There is also evidence showing the high photosynthetic activity in C_4 leaves can lead to the accumulation of higher levels of sugars, relative to C_3 species (Henry *et al.* 2020). Carbohydrate synthesis, metabolism and export differ in several ways between C_4 and C_3 photosynthetic species. As

mentioned, sucrose and starch synthesis is compartmentalised in leaves of C_4 grasses (Lunn and Furbank 1999). In addition, large metabolite pools are required to maintain high concentration gradient across the mesophyll-bundle sheath interface with higher plasmodesmatal connections in C_4 grasses, allowing fast metabolite exchange and efficient carbon concentration to Rubisco (Leegood 2002; Danila *et al.* 2016). Part of the 3-phosphoglycerate (PGA) produced by the Calvin cycle in bundle sheath cells is reduced in mesophyll cells due to lower photosystem II activity in the bundle sheath. Furthermore, there have been recent evidence that suggests that C_4 grasses have evolved sugar transporters, using a different strategy compared to C_3 grasses (Emms *et al.* 2016; Bezrutczyk *et al.* 2018; Hua *et al.* 2022; Chen *et al.* 2022). These factors suggest that sugar sensing may differ between C_4 and C_3 plants, and between the mesophyll and bundle sheath cells.

Three putative sugar sensor kinase proteins are known; Target of Rapamycin (TOR), SNF1- related kinase 1 (SnRK1), hexokinase (HXK) and the sugar sensing metabolite trehalose-6-phosphate (T6P). TOR functions as a protein kinase and is a part of the TOR complex (TORC), which also includes RAPTOR (Regulatory-Associated Protein of TOR 1) and LST8 (Lethal with Sec Thirteen 8). These additional proteins can act as regulatory components of the TORC (Xiong and Sheen 2014). In *Arabidopsis thaliana*, it has been established that the glucose-TOR signalling network can regulate numerous essential processes (Xiong and Sheen 2012; Xiong *et al.* 2013). Hexokinase was one of the first proteins for which a direct link between sugar sensing and photosynthesis was established (Moore *et al.* 2003). Several homologs, such as AtHXK1 in Arabidopsis and OsHXK5 and OsHXK6 in rice (*Oryza sativa*), have been established as sugar sensor proteins (Moore *et al.* 2003; Cho, Ryoo, Eom, *et al.* 2009). There has also been evidence for SnRK1 as a sugar sensing protein in plants (Jossier *et al.* 2009). The SnRK1 complex (SnRK1C) is made up of four subunits: the catalytic subunit (α), two regulatory subunits (β,γ) and a hybrid plant-specific subunit (βγ) and can be involved

in plant-pathogen interactions (Bouly *et al.* 1999; Lumbreras *et al.* 2001; Gissot *et al.* 2005, 2006). SnRK1 is thought to be upregulated when conditions are unfavourable for the plant (Baena-González *et al.* 2007; Zhang *et al.* 2009). There has been some evidence that SnRK1 is involved in the regulation of photosynthesis genes as the overexpression of *KIN10* (the gene encoding the SnRK catalytic subunit in Arabidopsis) causes a downregulation of photosynthetic genes. Furthermore, SnRK1 is inhibited by T6P(the precursor to the disaccharide trehalose), but not by other sugars. In plants, T6P can only be made when sufficient levels of sucrose are present (Lunn *et al.* 2006), and therefore acts as a signalling molecule for sucrose and correlates with active growth (Schluepmann *et al.* 2003; Martínez-Barajas *et al.* 2011; Lunn *et al.* 2014). (Lunn *et al.* 2006) Trehalose phosphate synthase (TPS) is responsible for the synthesis of T6P, and T6P can subsequently be converted to trehalose via trehalose phosphate phosphatase (TPP) (Ponnu *et al.* 2011; Paul *et al.* 2020). Trehalose can then be broken back down into its glucose units by trehalase (TRE). While trehalose is found at relatively low levels in plants, it is thought that trehalose metabolism plays an important regulatory role (Goddijn and Smeekens 1998).

Due to innate differences and the complexity of the signalling network, it is plausible to hypothesise that photosynthetic types may sense sugars differently. Sugar sensors may have evolved to accommodate the two-cell compartmentalisation of C_4 photosynthesis. In this study, publicly available transcriptome data from C_3 and C_4 grasses were used to investigate the expression of putative genes encoding components of each sugar sensor. The overall aim was to determine if there were differences in expression patterns between C_3 and C_4 grasses that might alter how sugar is perceived. Data were used to; 1) determine if there were C_4-specific residues in the sugar sensing genes associated with the evolution of C_4 photosynthesis; 2) compare the transcript abundance between the leaf (source) and seed (sink) in C_4 and C_3 grasses; and 3) along the leaf gradient of C_4 and C_3 grasses, where a single leaf undergoes a sink (base)-source (tip) transition during development (Jones and Eagles 1962; Turgeon and

Webb 1976; Harn *et al.* 1993; Kölling *et al.* 2013; Wang *et al.* 2014; Chen *et al.* 2022) 4) as well as between the bundle sheath and mesophyll cells of C_4 grasses to investigate whether there was preferential expression to one photosynthetic cell type. This approach can shed light on those sugar sensors that might be linked with photosynthesis (source tissue).

Materials and Methods

C_4 and C_3 grass species utilised

Sequences, transcript expression data, or both were extracted from eight C_4 grasses (*Panicum hallii*, *Panicum miliaceum*, Panicum antidotale, *Sorghum bicolor*, *Setaria italica*, *Setaria viridis*, *Saccharum spontaneum*, and *Zea mays*) and six C_3 grasses (*Steinchisma laxum*, *Hymenachne amplexicaulis*, *Cyrtococcum patens*, *Panicum bisulcatum*, *Brachypodium distachyon* and *Oryza sativa*). Which species, transcriptomes and raw RNA sequencing data used for each aspect of this study is summarised in Supplementary Data Table S1.

Obtaining and mining publicly available assemblies

Where genomes were publicly available, the associated annotations and transcriptomes were obtained and mined for genes of interest. Data were downloaded from Phytozome v13 (Goodstein *et al.*, 2012) or https://www.ncbi.nlm.nih.gov/ for the following assemblies: *Z. mays* v4 (Jiao *et al.* 2017), *S. spontaneum* (Zhang *et al.* 2018), *S. bicolor* v3.1.1 (McCormick *et al.* 2018), *S. italica* v2.2 (Bennetzen *et al.* 2012; Zhang *et al.* 2012), *S. viridis* v2.1 (Bennetzen *et al.* 2012), *P. hallii* v3.2 (Lovell *et al.* 2018), *O. sativa* v7 (Ouyang *et al.* 2007), *B. distachyon* v2.1 (Vogel *et al.* 2010). Known protein sequences from Arabidopsis, *Z. mays* and/or *O. sativa* were used to identify homologues in the other species through Phytozome v13 online interface (http://phytozome.jgi.doe.gov; Goodstein *et al.*, 2012). The gene IDs for each of the sequences from each species can be found in Supplementary Data File S1.

De novo assembly of RNA-Sequencing reads

A *de novo* transcriptome assembly was built for those species that had no publicly available genomes at the time of analysis using published RNA-sequencing (RNA-Seq) data. All RNA-Seq data sets were obtained from https://www.ncbi.nlm.nih.gov/ or https://www.ebi.ac.uk/ using the project's associated accession number **[Supplementary Data Table S1]**. Adapter sequences were first removed from all RNA-Seq reads using Trimmomatic (Bolger *et al.* 2014). The Trinity default pipeline was then implemented to create the *de novo* assemblies, each consisting of set of contiguous sequences (contigs) for each species (Grabherr *et al.* 2011; Haas *et al.* 2013). For each *de novo* assembly, annotation of contigs was required to identify genes of interest. For this, *de novo* assemblies were loaded into Geneious Prime 2022.2 (https://www.geneious.com; Kearse *et al.*, 2012), and nucleotide databases were created using the inbuilt NCBI BLAST tool. The NCBI tool within Geneious Prime 2022.2 was then used to carry out blastn queries, using sequences of genes of interest from *S. viridis* (Bennetzen *et al.* 2012) and *O. sativa* (Ouyang *et al.* 2007) transcriptomes, for identification.

Estimation of transcript abundance

RNA-Seq reads obtained **[Supplementary Data Table S1]** were quantified using the quasi-align mode in Salmon (Patro *et al.* 2017). A mapping-based index was created for each transcriptome or *de novo* transcriptome. Trimmed reads were then mapped to the relevant index using the default settings of the quant command in mapping-based mode within Salmon. This produced a normalised of transcripts per million (TPM) values for each transcript or contig (Kearse *et al.* 2012).

Protein sequence alignment and phylogeny

Protein alignments and phylogenetic trees were created to visualise homology using Geneious Prime 2022.2 (https://www.geneious.com; Kearse *et al.*, 2012). Alignments were created using Multiple Alignment with Fast Fourier Transform (MAFFT) using a G-INS-i algorithm and BLOSUM62 matrix (with a 1.53 gap penalty and 0.123 offset value) for the scoring (Katoh and Standley 2013). Phylogenetic trees were built using Randomized Axelerated Maximum Likelihood (RaxML) using 1000 bootstrap replicates (Stamatakis 2006, 2014).

Positive selection analysis using CodeML

To investigate for evidence of positive selection in genes of interest, CodeML was implemented to test residues for selection (Zhang *et al.* 2005). For this analysis, species were selected to ensure C_4 lineages were dispersed phylogenetically between C_3 species **[Supplementary Data Table S1]**. Phylogenetic trees created using RaxML were processed as Newick files and annotated (using #1 to denote a foreground branch) to test the hypothesis of selection in foreground branches. Those branches labelled as foreground were those which contain a C_4 species, hence, the following analyses test whether there is any positive selection associated with the evolution of C_4 photosynthesis (C_4 specific selection). CodeML was then used to test the ratio of non-synonymous to synonymous substitutions (dN/dS ratio; omega) under two scenarios. 1) A null model where all codons evolve under either purifying selection (omega < 1) or relaxed selection (omega = 1). 2) Sites evolve under purifying or neutral selection in the whole tree, except for foreground branches, where they evolve under positive selection (omega > 1). These scenarios were compared to estimate the posterior probability of each base evolving under positive selection using a Bayes empirical model. These scenarios were tested in pamlX, a package housing CodeML (Xu and Yang 2013).

Source to sink expression data

Publicly available transcript expression data from the leaf and seed was downloaded for two C_4 grasses and two C_3 grasses **[Supplementary Data Table S1]**. Except for data associated with *P. miliaceum,* all data were microarray data, where expression was represented as Robust Multichip Average (RMA)-normalised expression values. For *P. miliaceum,* the dataset was RNA-Seq, and therefore, TPM values were extracted as per above. Using these data, the leaf expression values were divided by the seed expression values to obtain a "source:sink" ratio. There were three biological replicates used for each study. Since there were only two species surveyed for each photosynthetic type, the biological replicates were used for the "n" when representing the source:sink ratio for C_4 and C_3 grasses. Therefore n=6 for the ratios in this experimental study. These values can be found in Supplementary Data File S2.

Leaf gradient expression data

Publicly available RNA-Seq data of leaf gradients were mined from four C_4 grasses and two C_3 grasses **[Supplementary Data Table S1]**. TPM values were extracted as per above. The expression profiles were represented as mean $\log_2$ TPM values for at least 3 biological replicates (except for *S. viridis* which had only one biological replicate). For each species between 5 – 15 leaf sections were segmented and sampled for RNA-Seq analysis. These values can be found in Supplementary Data File S3.

Bundle sheath and mesophyll cell expression data

RNA-Seq data were obtained from the bundle sheath and mesophyll cells of several C_4 grasses **[Supplementary Data Table S1]**. TPM values were extracted as per above. Each study had at

least three biological replicates for both cell types. The expression of genes is represented as TPM compared between the bundle sheath and mesophyll cells for each species. The TPM values were also averaged across all the C_4 grasses that were surveyed for each cell type. These values can be found in Supplementary Data File S4.

Data analysis

Figures and statistical analyses were performed using GraphPad Prism v9.4.1. A paired Student's t-test was used to compare the leaf to seed expression ratios of each sugar sensor gene to determine if it there was preferential expression to the "source" or "sink" tissue **[Supplementary Data Table S2]**. A paired Student's t-test was also carried out to compare the expression between bundle sheath and mesophyll cells of sugar sensor genes in C_4 grasses **[Supplementary Data Table S3]**.

Results

Identification of genes encoding sugar sensor components in C_4 and C_3 grasses

Identification of putative sugar sensors across selected C_4 and C_3 grasses was first carried out using BLAST searches of the respective genomes using known sequences from either *Z. mays* or Arabidopsis. Extracted sequences were translated and phylogenetic trees built to visualise homology to each other **[Supplementary Fig. S1-S6]**. Sequences from *Z. mays*, *S. spontaneum*, *S. bicolor*, *S. viridis*, *S. italica*, *P. miliaceum*, *P. hallii*, *O. sativa* and *B. distachyon* were extracted from their respective genomes where present.

Table 1 summarises the sugar sensor genes that were present or absent in each grass species. The *B. distachyon* genome did not contain a copy of RAPTOR2 and some grasses did not have a copy of RAPTOR3. Several grasses, such as *Z. mays*, *P. miliaceum* and *S. spontaneum*, also contained a second hybrid subunit within their genomes **[Supplementary Data Fig. S4]**. The number of hexokinase homologues varied between 6 – 9 across the grasses analysed **[Supplementary Data Fig. S5]**. Each genome contained a copy of HXK5 and a HXK6, the putative sugar sensors. Each species also contained a copy of TPS1, TPP and TRE **[Supplementary Data Fig. S6]**. Analysis of C_4 and C_3 grasses did not appear to show gene duplication during evolution.

Positive selection analyses were carried out for each putative sugar sensor using the extracted protein sequences to determine if there was any detectable C_4-dependent evolution within the set of genes. Sequences used were from four C_4 grasses, *P. antidotale*, *S. bicolor*, *S. viridis* and *Z. mays;* and five C_3 grasses, *H. amplexicaulis*, *P. bisulcatum*, *S. laxum*, *O. sativa* and *C. patens*. Nicotinamide-adenine dinucleotide phosphate-malic enzyme (NADP-ME) was used as a control for these analyses as it is known that several residues of this gene are under C_4 specific

selection. As expected, several residues were identified as being under C_4 specific selection in NADP-ME **[Supplementary Data Fig. S7]**. However, no residues were identified as being under C_4 specific selection within any of the sugar sensor proteins tested here (TOR, LST8-1, RAPTOR1, RAPTOR2, SnRK1α, β, γ, βγ subunits, HXK5, HXK6, TPS1, TPP1 and TRE).

Sugar sensor genes are expressed in both the source and sink tissues of C_4 and C_3 grasses

Source (leaf) and sink (seed) transcriptomic data were scrutinised to determine whether differences at the gene expression level are associated with the evolution of C_4 photosynthesis (Fig. 1; **Supplementary Data File S1**). Using publicly available leaf and seed transcriptomic data, gene expression of sugar sensor genes were extracted for two C_4 grasses (*Z. mays* and *P. miliaceum*) and two C_3 grasses (*O. sativa* and *B. distachyon*) (Jain *et al.* 2007; Sekhon *et al.* 2011; Yue *et al.* 2016; Sibout *et al.* 2017). Data was combined for each photosynthetic type for analysis. Within these datasets, *TOR* was not in either of the datasets for the C_4 grasses, and RAPTOR*3* expression was not detected in the C_3 grass *B. distachyon*. Genes encoding the TORC subunits exhibited heightened transcript expression in the leaves (source tissue) of C_3 grasses, when compared to the ratios exhibited by C_4 grasses. The source to sink ratio for the C_4 grasses were close to one for many of the sugar sensing genes, suggesting they are expressed equally between leaf and seed tissues, at least for these grasses. Only genes encoding the regulatory subunit of SnRK1C (*SnRK1βγ1*) and *TPP1* (which encodes the trehalose phosphate phosphatase enzyme) had significantly higher ($P \leq 0.05$) expression in the leaf compared to the seed for the C_3 grasses. There was no significant expression of any gene for the C_4 species or towards the seed (i.e. <1 and significantly different to 1). It can also be noted that *HXK5* source to sink ratio was ~5.6-fold higher for the C_3 grasses than the C_4 grasses, and this change was

even more apparent for HXK6 gene expression at an ~58.3-fold difference. However, these differences were not identified as significant.

There were more significant changes ($P \leq 0.05$) within individual species that indicate some sugar sensor genes may be preferentially expressed in the source or sink tissues **[Supplementary Data Fig. S8]**. Notably, many genes identified as significantly different in *Z. mays* had a ratio <1, indicating higher amounts of transcripts were identified in the sink tissues. Preferential expression to either the leaf or seed is more prominent within a species rather than collectively as a photosynthesis type **[Supplementary Fig. S1]**.

Sugar sensor genes are largely stably expressed along the leaf gradient of C_3 and C_4 grasses

Publicly available RNA-Seq data were mined for their expression along the leaf gradient of various C_3 and C_4 grasses and represented as heatmaps (Li *et al.* 2010; Wang *et al.* 2014; Ding *et al.* 2015; Hu *et al.* 2018) (Fig. 2-5). This analysis was carried out to determine whether there were possible changes in sugar sensing along the leaf and/or between C_4 and C_3 grasses during the sink to source transition from the base to the tip. The expression profiles for the genes encoding TORC subunits are displayed for *TOR*, *LST8-1*, *RAPTOR1* and *RAPTOR2* (Fig. 2A-D). *RAPTOR3* was excluded since this subunit was only found in some species. Notably, *B. distachyon* orthologues were expressed at high levels compared to the other grasses. Further, *LST8-1* and RAPTOR2 transcripts were also highly abundant along the leaf gradient in *S. spontaneum* and *S. bicolor*.

Similarly, to genes that encode TORC subunits, the expression profiles of genes that encode the SnRK1C subunits were also examined along the leaf gradient of these grasses (Fig. 3).

SnRK1γ2 and *SnRK1βγ2* were excluded from the heatmaps because they were absent in multiple genomes. The α subunits were found to be expressed in all species examined to varying levels (Fig. 3A-C). Expression was largely stable across the leaf in each species; however, some patterns were apparent. The genes encoding the α subunits of *S. bicolor* generally had higher expression toward the tip of the leaf. A similar pattern was observed for *SvSnRK1α1*. Conversely, *SsSnRK1β2* and *ZmSnRK1β3* were expressed higher at the base of the leaf. In the mid sections of the leaf, *SvSnRK1β2* and *SsSnRK1γ1* were expressed at higher levels.

The expression of the genes encoding putative sugar sensors *HXK5* and *HXK6* were examined to investigate whether glucose sensing may differ across the leaf gradient in C_4 and C_3 grasses (Fig. 4). *HXK5* was expressed at high levels for all species except for *Z. mays* (Fig. 4A). Notably, for several C_4 grasses (*S. spontaneum*, *S. bicolor* and *S. viridis*) higher expression tended toward the base of the leaf for *HXK5*. Despite high homology between *HXK5* and *HXK6*, *HXK6* was largely expressed at low levels (Fig. 4B). Only S. *viridis* and *B. distachyon* exhibited high abundance of *HXK6* transcripts (Fig. 4B).

Finally, genes encoding enzymes associated with trehalose metabolism were interrogated along the leaf gradient. Similarly, to many other genes encoding sugar sensing components, *TPS1*, *TPP* and *TRE* transcripts were expressed at varying degrees across the leaf and between species (Fig. 5). For *SbTPS1*, leaf sections 8 – 10 (around the middle) exhibited the highest transcript expression compared to the rest of the leaf (Fig. 5A). *SsTPP* was expressed relatively ubiquitously along the leaf at high levels, while *SvTPP* and *ZmTPP* were preferentially expressed at the base of the leaf (Fig. 5B). *SbTRE* was highly expressed when compared to the other grasses, especially toward the tip of the leaf (Fig. 5C).

Sugar sensor genes exhibit species-specific preferential expression to either bundle sheath or mesophyll cells

Transcript expression associated with sugar sensing genes was analysed within bundle sheath and mesophyll cells of several C_4 grasses from publicly available RNA-Seq datasets (John *et al.* 2014; Döring *et al.* 2016; Denton *et al.* 2017; Washburn *et al.* 2021). These results are presented for *Z. mays*, *S. bicolor*, *S. viridis*, *S. italica* and *P. hallii* (Fig. 6, **Supplementary Data File S4, Supplementary Data Table S3**). Datasets from C_3 grasses were not examined in this study since they were sparse or had poor mapping of reads to their respective genomes, likely due to the difficulty of isolating and separating these cells in C_3 species.

In *Z. mays*, sugar sensors genes were generally not preferentially expressed in one photosynthetic cell type (Fig. 6A). *ZmSnRK1β3* showed the highest overall expression out of all the genes surveyed, while *ZmTPP* was significantly higher ($P \leq 0.05$) in the mesophyll cell. Unlike *Z. mays*, in *S. bicolor* and *P. hallii* there were numerous significant differences ($P \leq 0.05$) in transcript expression of sugar sensor genes, with almost all those identified as significant being elevated in bundle sheath cells (Fig. 6B,C). All genes encoding the TORC subunits (except *PhLST8-1*) and SnRK1α were shown to be significantly preferentially expressed in the bundle sheath cells of *S. bicolor* and *P. hallii*. Where the two species differed was the transcript expression of *SnRK1β1* and *SnRK1β3*, which were expressed preferentially in mesophyll cells of *P. hallii*, but not *S. bicolor*. The largest fold change shifts were for *TPS1*, for which there was a 27- and 15-fold change increase in bundle sheath cells in *S. bicolor* and *P. hallii*, respectively. *S. viridis* and *S. italica* are two close relatives within the millets. Both species exhibited less significant differences in sugar sensor gene expression between the two photosynthetic cell types when compared to *S. bicolor* (Fig. 6D,E). In addition, unlike *S.*

bicolor, numerous genes had significantly higher ($P \leq 0.05$) expression in mesophyll cells of both or one of the species. Transcript expression of LST8-1 was significantly elevated in mesophyll cells of both *S. viridis* and *S. italica*. Several genes encoding the SnRK1C subunits showed significant differences in transcript expression between the two cells; *SvSnRK1α3* and *SvSnRK1β2* with preference to the bundle sheath and mesophyll, respectively. *SiSnRK1α1* exhibited significantly elevated expressed in the mesophyll cells, although this was reversed for the other two *SiSnRK1α* subunit genes. Similar to *S. bicolor* and *P. halli*, there was also significant ~29.7- and ~47.3 -fold increases in expression of *TPS1* in bundle sheath cells of *S. viridis* and *S. italica*, respectively.

The values for all sugar sensor genes examined were averaged and the resulting log_2 TPM values and visualised for each cell type (Fig. 6F). Within this analysis, only *SnRK1β1* and *TPS1* transcript expression was significantly different between the bundle sheath and mesophyll cells **[Supplementary Data Table S3]**. The average *SnRK1β1* expression was higher in mesophyll cells for the C_4 grasses examined, however, the fold differences were small. Although not significant, generally there was higher transcript abundance within the bundle sheath cell for *SnRK1α2*, *SnRK1α3*, *SnRK1γ1*, *HXK5* and *HXK6*. Like with the source to sink expression comparison, significant changes within a species were more common than significant changes associated with photosynthetic type.

Discussion

No co-optional evolution for C_4 sugar sensors but some species-specific preferential expression in bundle sheath or mesophyll cells

In this study it was hypothesised that sugar sensors have evolved to accommodate the two-celled compartmentation of C_4 photosynthesis. To determine whether sugar sensors

diverged from their C_3 counterparts during the evolutionary transition from C_3 to C_4 photosynthesis, transcript sequences from C_4 species (*P. antidotale*, *S. bicolor*, *S. viridis* and *Z. mays*) and C_3 species (*H. amplexicaulis*, *P. bisulcatum*, *S. laxum*, *O. sativa* and *C. patens*) were utilised. No evidence for the positive selection of C_4 sugar sensors during C_4 evolution was identified within this study. This result was unexpected, as the evolution of C_4 photosynthesis has resulted in major changes, involving C_4 specific residue changes in numerous key genes (Christin *et al.* 2009; Watson-Lazowski *et al.* 2018). However, it is plausible that selection pressures associated with C_4 photosynthesis have not influenced the sugar sensors in this specific way. For example, it has been well-established that gene duplications have occurred during the evolution of C_4 photosynthesis but it was not observed for genes in this study (Marshall *et al.* 1996; Monson 1999, 2003). Moreover, changes to cis-regulatory elements in single copy genes have contributed to the altered expression patterns that facilitate C_4 photosynthesis (Rosche and Westhoff 1995). Aspects such as these may still facilitate C_4 specific expression patterns of sugar sensing genes.

When examining the general expression of the genes that encode the proteins that make up TORC there was little change between the bundle sheath and mesophyll cells of the C_4 grasses (Fig. 6). The expression of TOR varied between species and was not significantly expressed in one cell type over another when collectively examining the C_4 grasses, which suggests that the TOR protein has a signalling role in both cells. Studies in the algae *Chlamydomonas reinhardtii* have shown that CO_2 fixation promotes TOR activity but has no effect on TOR or LST8 protein abundance (Mallen-Ponce *et al.* 2022). Furthermore, it was observed that photosynthesis inhibition decreases TOR activity. The variation in gene expression for the subunits that encode TORC could be also related to the role it has in the circadian rhythm (Xiong and Sheen 2014; Dong *et al.* 2017). Therefore, tissue harvest time across studies could influence transcript abundance of the genes encoding TORC subunits.

Moreover, its role as a master regulator across different tissues and processes could also account for the lack of differences in gene expression between the two photosynthetic cell types when collectively analysing the C_4 grasses in this study (Pacheco *et al.* 2021). Sucrose and starch synthesis occurs in the mesophyll and bundle sheath cells of C_4 species, respectively. Although TORC is regulated by sugars, the complex also regulates starch accumulation. These observations could account for the presence of genes relating to this complex in both cell types.

Like TORC, SnRK1C is thought to regulate many processes, and is usually upregulated under stress conditions when sucrose availability is low (Baena-González *et al.* 2007). Although the data were generated from plants grown in normal conditions, the overall transcript abundance of genes encoding SnRK1C subunits were high in comparison to the other sugar sensors (Fig. 6). On average, within the C_4 grasses examined, *SnRK1β1* was preferentially expressed in mesophyll cells (Fig. 6F, **Supplementary Data Table S3**). *SnRK1β1* encodes a regulatory component of the complex and β subunits can be expressed at varying levels depending on the tissue, developmental stage and environmental cues (Polge *et al.* 2008). Therefore, it is a possibility that SnRK1β1 regulates the interaction of the kinase with its targets within the mesophyll cells of C_4 grasses. When averaged across the C_4 species surveyed, *SnRK1α* genes (which encode the catalytic subunit of the complex) were not significantly different between cells. Nevertheless, it must be noted that many of the grasses had higher expression within the bundle sheath cells of the *SnRK1α* catalytic subunit genes (Fig. 6B-E). There is a possibility that SnRK1α subunits are important for sensing and/or signalling during sucrose translocation, in which photoassimilates pass through the bundle sheath cells for phloem loading to occur (Bezrutczyk *et al.* 2018; Chen *et al.* 2022). During this process, genes encoding regulatory subunits may be expressed according to translocation needs and photosynthetic activity. Alternatively, expression in the bundle sheath cells could be linked to

a role in regulating genes associated with starch synthesis, which has been evidenced in the seed (Zhang *et al.* 2001; Tiessen *et al.* 2003).

As mentioned previously, T6P signalling has been closely linked with SnRK1C activity (Baena-González and Lunn 2020). *TPS1* expression was significantly higher in the bundle sheath cells when averaged across the C_4 grasses (Fig. 6F). TPS is involved in the synthesis of T6P, and its presence indicates elevated sucrose levels (Grennan 2007). Therefore, it was surprising that *TPS1* was higher in the bundle sheath cells, since sucrose biosynthesis occurs predominantly in the mesophyll cells of C_4 grasses (Lunn and Furbank 1999; Furbank and Kelly 2021). As suggested with SnRK1C, T6P signalling may play an important role in the phloem loading process, (Emms *et al.* 2016; Bezrutczyk *et al.* 2018, 2021; Chen *et al.* 2022). Interestingly, trehalose increases the expression of *ApL3* that encodes an ADP-glucose pyrophosphorylase that subsequently increases starch synthesis (Wingler *et al.* 2000). Therefore, the trehalose biosynthesis pathway maybe important for starch production within the bundle sheath cells of C_4 grasses. The additional genes encoding enzymes associated with T6P metabolism were expressed at similar levels between the bundle sheath and mesophyll cells for all species analysed. This could suggest that the synthesis, breakdown and signalling of trehalose is important in both cells, or since trehalose is a non-reducing disaccharide, it could also play a role in buffering sucrose loading into the phloem.

There were also differences in expression of the putative HXK sugar sensors, *HXK5* and *HXK6*, between the two photosynthetic cells for several C_4 species. For example, *SbHXK5*, *SbHXK6*, *PhHXK5* and *PhHXK6* were all expressed at higher levels in the bundle sheath compared to mesophyll cells (Fig. 6B,C). This could indicate that the phosphorylation of glucose is more prevalent in the bundle sheath cells of C_4 species, or that glucose sensing predominates there. Research on the effect of HXK sugar sensing in C_4 species has been sparse, but seminal studies using *Z. mays* protoplasts have shown that glucose, the substrate for HXK,

can repress photosynthesis genes (Sheen 1990; Jang and Sheen 1994). It must be noted that this was only examined in a single cell system and did not examine the whole leaf or how the plant that might affect how sugar sensing occurs, given photosynthesis takes place in a two-cell system in *Z. mays*.

Expression of sugar sensor genes changes in source-sink developmental models

To investigate the expression patterns of genes encoding sugar sensor components in source and sink tissues, leaf and seed tissues, as well as developmental leaf gradients, were interrogated to determine if there was preferential expression to the source or sink tissue. Given source to sink expression gradients have been observed with sugar transporters and other genes associated with sugar metabolism in C_4 grasses, it may be expected that similar expression patterns are found for genes encoding the sugar sensor proteins (Bezrutczyk *et al.* 2018; Hu *et al.* 2018; Chen *et al.* 2022).

As previously established, TORC is a master regulator of many different processes in the plant. Therefore, genes encoding this complex would more likely be found in all tissue types. For the C_4 species examined, gene expression of the regulatory subunits of TORC were close to one, whereas for the C_3 species, the expression of numerous TORC genes trended towards source tissue (ratio of <1) (Fig. 1). The expression of these genes was also ubiquitous along the leaf gradient of the four C_4 grasses and the two C_3 grasses (Fig. 2). Interestingly, it has been shown that when TORC repression is initiated, *S. viridis* showed a milder phenotype and a smaller magnitude of changes relating to primary metabolites and global gene expression, when compared to the C_3 Arabidopsis (da Silva *et al.* 2021). This might suggest that plant growth in C_4 species is less rigorously controlled by TORC, or is less sensitive to changes in carbon status. Previous work on the relationship between CO_2 fixation and TOR activity has

suggested that CO_2 fixation status can influence TOR activity, but not necessarily change the protein abundance (Mallen-Ponce *et al.* 2022). Thus, this might also mean that the transcript abundance of the subunits of TORC may not change between source and sink tissues, but rather activity is modulated via other factors.

Like TORC, SnRK1C is thought to regulate numerous processes throughout the plant. The seed to leaf expression ratio of genes encoding the catalytic subunits of SnRK1C for both C_4 and C_3 species were close to one, demonstrating that they are found in both the seed and leaf tissues of the analysed grasses (Fig. 1). This suggests that these genes play a similar role within the plant regardless of whether they are C_4 or C_3 species. When examining the expression of genes that encode subunits of SnRK1C over a leaf gradient, again there were no immediate trends that differentiate source to sink or C_4 and C_3 leaves along the leaf gradient (Fig. 3). This data would suggests that SnRK1 is largely equally distributed across source and sink tissue of C_3 and C_4 grasses. . However, SnRK1C is known to be activated in response to unfavourable conditions or during a starvation response (Baena-González *et al.* 2007). Therefore, the lack of differences between source and sink tissues might not be uncommon since these plants were grown in normal conditions. In addition, there is evidence that SnRK1α is regulated on the posttranscriptional level (Lu *et al.* 2007), which may also explain the limited differences identified...

While the link between photosynthesis and SnRK1C is not well documented, a direct link between HXK sugar sensing and modulating photosynthesis gene expression has been identified. This was first established using *Z. mays* protoplasts, as mentioned previously (Sheen 1990; Jang and Sheen 1994). This was later confirmed using *gin2* mutants of Arabidopsis, showing AtHXK1 could sense glucose, and in turn influence photosynthesis gene expression (Moore *et al.* 2003). Sugar sensors have also been established in rice (C_3 grass) via overexpression lines of OsHXK5 and OsHXK6, which exhibited heightened sensitivity to

glucose (Cho *et al.* 2006; Cho, Ryoo, Hahn, *et al.* 2009). These rice lines were generally smaller than WT and showed decreased expression of key photosynthesis genes, such as the Rubisco small subunit gene (*rbcS*). The homologues of HXK5 and HXK6 were expressed in both the leaf and seed tissues of the C_4 and C_3 species examined (Fig. 1). The source-sink ratio for C_4 grasses was close to one, whereas for C_3 grasses, it was well above one. Although these differences were not significant within our dataset, the extent of the differences would suggest that HXKs predominates in the leaves of C_3 grasses. Expression of *HXK5* and *HXK6* homologues was apparent all along the leaves of both C_4 and C_3 grasses, and changes along the leaf were subtle (Fig. 4). This is unlike sugar transporters and starch and sugar metabolism genes, which exhibited a more prominent gradient as the tissue changes from sink to source from the base to the tip of the leaf (Chen *et al.* 2022). For *HXK5*, there was higher abundance at the base of the leaf, where it is more sink-like tissue, for the C_4 grasses *S. spontaneum*, *S. bicolor* and *S. viridis* (Fig. 4A). This may suggest a role in sensing incoming photoassimilates that break down to glucose for utilisation as the tissue matures. However, like TOR and SnRK1α, HXK sugar sensors could also be post-transcriptionally regulated, and so changes in expression may be minor and not correlate with activity.

T6P abundance is thought to modulate SnRK1C activity, subsequently de-repressing anabolic processes (Baena-González *et al.* 2007; Lawlor and Paul 2014). SnRK1C is known to be involved in starch synthesis during grain filling of grasses by regulating the expression of genes encoding proteins involved in this process, and there has also been suggestions that its activity is controlled by T6P levels (Laurie *et al.* 2003; Lu *et al.* 2007; Gazzarrini and Tsai 2014). In this study, the *TPP1* source to sink expression ratio was significantly above one for C_3 grasses, which may suggest that T6P (or trehalose itself) have a larger role in sugar sensing and signalling within the leaves (Fig. 1). The transgenic manipulation of *TPP1* in *Z. mays* showed that T6P plays a large role in coordinating photoassimilate partitioning to the

reproductive tissues by regulating photosynthesis (Oszvald *et al.* 2018). The authors showed that *Sugars Will Eventually be Exported Transporters* (*SWEET*) genes were upregulated in the transgenic lines, increasing the movement of photoassimilates to sink tissue, particularly under drought conditions. Other genes associated with T6P metabolism also had source to sink ratios above one in this study, although these differences were not significant. Further analysis on the expression of these genes along the leaf gradient of C_4 and C_3 grasses showed that they were expressed throughout, and many only showed small changes from the base to the tip (Fig. 5).

Conclusions

In this study, transcriptomic data across various C_4 and C_3 grasses were analysed to determine gene expression patterns of the components of TORC, SnRK1C and HXK sugar sensors, as well as T6P metabolism. These analyses focused on the role these sugar sensors in relation to photosynthesis, where sugars are produced, and whether sugars may be perceived differently between C_4 and C_3 grasses. Even though C_3 grasses perform photosynthetic and carbohydrate production reactions in one cell type, unlike C_4 grasses which is compartmentalised, not many changes in sugar sensor gene expression were observed between the two types of plants.

There were few distinct gradient transitions of expression for sugar sensor genes, suggesting sugar sensing is important along the whole young leaf. Moreover, when expression was examined in the two photosynthetic cell types in C_4 grass leaves only, *SnRK1β1* and *TPS1* were preferentially expressed in the mesophyll and bundle sheath cells, respectively. Although, it must be noted that within species there were more distinct changes in expression of each sugar sensor gene.

Future studies could be incorporated to analyse sugar sensors between C_4 and C_3 grasses by examining protein abundance and activity to determine if sugars are perceived differently.

These studies can also be expanded into a larger variety of C_4 and C_3 species that include dicots and monocots and different sub-types of C_4 photosynthesis. Nevertheless, this study provides a foundation for which the role of sugar sensors can be scrutinised, especially in terms of how it may relate to C_4 and C_3 photosynthesis.

Supplementary Data

Figure S1 Phylogenetic tree of monocot TOR complex subunits.

Figure S2 Phylogenetic tree of monocot SnRK1α subunits.

Figure S3 Phylogenetic tree of monocot SnRK1β subunits.

Figure S4 Phylogenetic tree of monocot SnRK1βγ and SnRK1γ subunits.

Figure S5 Phylogenetic tree of monocot hexokinases.

Figure S6 Phylogenetic tree of monocot proteins related to T6P metabolism.

Figure S7 C_4-dependent evolution of NADP-ME.

Figure S8 Leaf to seed expression ratio of sugar sensor genes in C_4 and C_3 grasses.

Table S1 Summary of species used in this study, data accession numbers and references.

Table S2 Leaf to seed expression ratio of sugar sensor genes in C_4 and C_3 grasses.

Table S3 Bundle sheath and mesophyll cell sugar sensor gene expression in C_4 grasses.

Supplementary Data File S1 Gene IDs.

Supplementary Data File S2 Leaf to seed expression ratios of C_4 and C_3 grasses.

Supplementary Data File S3 Leaf gradient expression of sugar sensors from C_4 and C_3 grasses.

Supplementary Data File S4 Bundle sheath and mesophyll expression of sugar sensors from C_4 and C_3 grasses.

Acknowledgements

OG, RTF and AWL designed the experiment; UB processed the raw reads of the RNAseq data and created the phylogenetic trees under supervision of AWL. LC constructed the Figures and wrote the manuscript with contribution from all authors.

Funding

This work was funded by the ARC Centre of Excellence for Translational Photosynthesis (Grant Number CE140100015) and ARC Discovery Project (DP210102730) awarded to OG and RTF.

Conflict of Interest

The authors declare no conflicts of interest.

Literature Cited

Baena-González E, Lunn JE. **2020**. SnRK1 and trehalose 6-phosphate – two ancient pathways converge to regulate plant metabolism and growth. *Current Opinion in Plant Biology* **55**: 52–59.

Baena-González E, Rolland F, Thevelein JM, Sheen J. **2007**. A central integrator of transcription networks in plant stress and energy signalling. *Nature* **448**: 938–942.

Bennetzen JL, Schmutz J, Wang H, *et al.* 2012. Reference genome sequence of the model plant Setaria. *Nature Biotechnology* **30**: 555–561.

Bezrutczyk M, Hartwig T, Horshman M, *et al.* 2018. Impaired phloem loading in *zmsweet13a,b,c* sucrose transporter triple knock-out mutants in *Zea mays*. *New Phytologist* **218**: 594–603.

Bezrutczyk M, Zöllner NR, Kruse CPS, *et al.* 2021. Evidence for phloem loading via the abaxial bundle sheath cells in maize leaves. *Plant Cell* **33**: 531–547.

Blechschmidt-Schneider S, Ferrar P, Osmond CB. **1989**. Control of photosynthesis by the carbohydrate level in leaves of the C_4 plant *Amaranthus edulis* L. *Planta 1989 177:4* **177**: 515–525.

Bolger AM, Lohse M, Usadel B. **2014**. Trimmomatic: a flexible trimmer for Illumina sequence data. *Bioinformatics* **30**: 2114–2120.

Bouly JP, Gissot L, Lessard P, Kreis M, Thomas M. **1999**. *Arabidopsis thaliana* proteins related to the yeast SIP and SNF4 interact with AKINα1, an SNF1-like protein kinase. *The Plant Journal* **18**: 541–550.

Von Caemmerer S, Furbank RT. **2003**. The C_4 pathway: An efficient CO_2 pump. *Photosynthesis Research* **77**: 191–207.

Chen L, Ganguly DR, Shafik SH, *et al.* 2022. Elucidating the role of SWEET13 in phloem loading of the C4 grass Setaria viridis. *The Plant Journal* **109**: 615–632.

Cho J Il, Ryoo N, Eom JS, *et al.* 2009. Role of the rice hexokinases OsHXK5 and OsHXK6 as glucose sensors. *Plant Physiology* **149**: 745–759.

Cho J Il, Ryoo N, Hahn TR, Jeon JS. **2009**. Evidence for a role of hexokinases as conserved glucose sensors in both monocot and dicot plant species. *Plant Signaling and Behavior* **4**:

908–910.

Cho J Il, Ryoo N, Ko S, *et al.* 2006. Structure, expression, and functional analysis of the hexokinase gene family in rice (*Oryza sativa* L.). *Planta* **224**: 598–611.

Christin PA, Osborne CP. **2014**. The evolutionary ecology of C_4 plants. *New Phytologist* **204**: 765–781.

Christin PA, Petitpierre B, Salamin N, Büchi L, Besnard G. **2009**. Evolution of C_4 phosphoenolpyruvate carboxykinase in grasses, from genotype to phenotype. *Molecular Biology and Evolution* **26**: 357–365.

Danila FR, Quick WP, White RG, Furbank RT, von Caemmerer S. **2016**. The metabolite pathway between bundle sheath and mesophyll: Quantification of plasmodesmata in leaves of C_3 and C_4 monocots. *The Plant Cell* **28**: 1461–1471.

Danila FR, Quick WP, White RG, Kelly S, Von Caemmerer S, Furbank RT. **2018**. Multiple mechanisms for enhanced plasmodesmata density in disparate subtypes of C_4 grasses. *Journal of Experimental Botany* **69**: 1135–1145.

Danila FR, Thakur V, Chatterjee J, *et al.* 2021. Bundle sheath suberisation is required for C_4 photosynthesis in a *Setaria viridis* mutant. *Communications Biology* **4**: 1–10.

Dengler NG, Nelson T. **1999**. Leaf structure and development in C_4 plants In: Sage RF, Monson RK, eds. *C4 Plant Biology*. Dan Diego: Academic Press, 133–172.

Denton AK, Maß J, Külahoglu C, Lercher MJ, Bräutigam A, Weber APM. **2017**. Freeze-quenched maize mesophyll and bundle sheath separation uncovers bias in previous tissue-specific RNA-Seq data. *Journal of Experimental Botany* **68**: 147–160.

Ding Z, Weissmann S, Wang M, *et al.* 2015. Identification of photosynthesis-associated C_4 candidate genes through comparative leaf gradient transcriptome in multiple lineages of C_3

and C_4 species. *PLOS ONE* **10**: e0140629.

Dong Y, Silbermann M, Speiser A, *et al.* 2017. Sulfur availability regulates plant growth via glucose-TOR signaling. *Nature Communications 2017 8:1* **8**: 1–10.

Döring F, Streubel M, Bräutigam A, Gowik U. **2016**. Most photorespiratory genes are preferentially expressed in the bundle sheath cells of the C_4 grass *Sorghum bicolor*. *Journal of Experimental Botany* **67**: 3053–3064.

Emms DM, Covshoff S, Hibberd JM, Kelly S. **2016**. Independent and parallel evolution of new genes by gene duplication in two origins of C_4 photosynthesis provides new insight into the mechanism of phloem loading in C_4 species. *Molecular Biology and Evolution* **33**: 1796–1806.

Furbank R, Hatch M. **1987**. Mechanism of C_4 photosynthesis: The size and composition of the inorganic carbon pool in bundle sheath cells. *Plant Physiology* **85**: 958–964.

Furbank RT, Kelly S. **2021**. Finding the C_4 sweet spot: cellular compartmentation of carbohydrate metabolism in C_4 photosynthesis. *Journal of Experimental Botany* **72**: 6018–6026.

Gazzarrini S, Tsai AY-L. **2014**. Trehalose-6-phosphate and SnRK1 kinases in plant development and signaling: the emerging picture. *Frontiers in Plant Science* **5**: 119.

Ghannoum O, Caemmerer S Von, Ziska LH, Conroy JP. **2000**. The growth response of C_4 plants to rising atmospheric CO_2 partial pressure: a reassessment. *Plant, Cell & Environment* **23**: 931–942.

Gissot L, Polge C, Bouly JP, Lemaitre T, Kreis M, Thomas M. **2005**. AKINβ3, a plant specific SnRK1 protein, is lacking domains present in yeast and mammals non-catalytic β-subunits. *Plant Molecular Biology 2005 56:5* **56**: 747–759.

Gissot L, Polge C, Jossier M, *et al.* 2006. AKINβγ contributes to SnRK1 heterotrimeric complexes and interacts with two proteins implicated in plant pathogen resistance through its KIS/GBD sequence. *Plant Physiology* **142**: 931.

Goddijn O, Smeekens S. **1998**. Sensing trehalose biosynthesis in plants. *The Plant Journal* **14**: 143–146.

Goodstein DM, Shu S, Howson R, *et al.* 2012. Phytozome: a comparative platform for green plant genomics. *Nucleic Acids Research* **40**: D1178-86.

Gowik U, Burscheidt J, Akyildiz M, *et al.* 2004. cis-Regulatory elements for mesophyll-specific gene expression in the C_4 plant Flaveria trinervia, the promoter of the C_4 phosphoenolpyruvate carboxylase gene. *The Plant Cell* **16**: 1077–1090.

Grabherr MG, Haas BJ, Yassour M, *et al.* 2011. Full-length transcriptome assembly from RNA-seq data without a reference genome. *Nature biotechnology* **29**: 644–52.

Grennan AK. **2007**. The role of trehalose biosynthesis in plants. *Plant Physiology* **144**: 3.

Haas BJ, Papanicolaou A, Yassour M, *et al.* 2013. *De novo* transcript sequence reconstruction from RNA-seq using the Trinity platform for reference generation and analysis. *Nature Protocols 2013 8:8* **8**: 1494–1512.

Haberlandt G. **1904**. *Physiologische Pflanzenanatomie*. Leipzig: Wilhelm Engelmann.

Harn C, Khayat E, Daie J. **1993**. Expression dynamics of genes encoding key carbon metabolism enzymes during sink to source transition of developing leaves. *Plant and Cell Physiology* **34**: 1045–1053.

Hatch MD. **1987**. C_4 photosynthesis: A unique blend of modified biochemistry, anatomy and ultrastructure. *Biochimica et Biophysica Acta (BBA) - Reviews on Bioenergetics* **895**: 81–106.

Hatch MD, Slack CR. **1966**. Photosynthesis by sugar-cane leaves. A new carboxylation reaction and the pathway of sugar formation. *The Biochemical Journal* **101**: 103–111.

Hattersley PW. **1984**. Characterization of C_4 type leaf anatomy in grasses (Poaceae). Mesophyll: bundle sheath area ratios. *Annals of Botany* **53**: 163–180.

Henry C, Watson-Lazowski A, Oszvald M, *et al.* 2020. Sugar sensing responses to low and high light in leaves of the C_4 model grass *Setaria viridis*. *Journal of Experimental Botany* **71**: 1039–1052.

Hibberd JM, Covshoff S. **2010**. The regulation of gene expression required for C_4 photosynthesis. *Annual Review of Plant Biology* **61**: 181–207.

Hu W, Hua X, Zhang Q, *et al.* 2018. New insights into the evolution and functional divergence of the *SWEET* family in Saccharum based on comparative genomics. *BMC Plant Biology* **18**: 270.

Hua X, Shen Q, Li Y, *et al.* 2022. Functional characterization and analysis of transcriptional regulation of sugar transporter *SWEET13c* in sugarcane *Saccharum spontaneum*. *BMC Plant Biology* **22**: 1–16.

Jain M, Nijhawan A, Arora R, *et al.* 2007. F-Box proteins in rice. Genome-wide analysis, classification, temporal and spatial gene expression during panicle and seed development, and regulation by light and abiotic stress. *Plant Physiology* **143**: 1467–1483.

Jang JC, Sheen J. **1994**. Sugar sensing in higher plants. *The Plant Cell* **6**: 1165–1179.

Jiao Y, Peluso P, Shi J, *et al.* 2017. Improved maize reference genome with single-molecule technologies. *Nature 2017 546:7659* **546**: 524–527.

John CR, Smith-Unna RD, Woodfield H, Covshoff S, Hibberd JM. **2014**. Evolutionary convergence of cell-specific gene expression in independent lineages of C_4 grasses. *Plant*

Physiology **165**: 62–75.

Jones H, Eagles JE. **1962**. Translocation of ^{14}Carbon within and between leaves. *Annals of Botany* **26**: 505–510.

Jossier M, Bouly JP, Meimoun P, *et al.* 2009. SnRK1 (SNF1-related kinase 1) has a central role in sugar and ABA signalling in *Arabidopsis thaliana*. *The Plant Journal* **59**: 316–328.

Katoh K, Standley DM. **2013**. MAFFT Multiple Sequence Alignment Software Version 7: Improvements in Performance and Usability. *Molecular Biology and Evolution* **30**: 772–780.

Kearse M, Moir R, Wilson A, *et al.* 2012. Geneious Basic: an integrated and extendable desktop software platform for the organization and analysis of sequence data. *Bioinformatics (Oxford, England)* **28**: 1647–9.

Kölling K, Müller A, Flütsch P, Zeeman SC. **2013**. A device for single leaf labelling with CO_2 isotopes to study carbon allocation and partitioning in *Arabidopsis thaliana*. *Plant Methods* **9**: 45.

Laurie S, McKibbin RS, Halford NG. **2003**. Antisense SNF1-related (SnRK1) protein kinase gene represses transient activity of an α-amylase (*α-Amy2*) gene promoter in cultured wheat embryos. *Journal of Experimental Botany* **54**: 739–747.

Lawlor DW, Paul MJ. **2014**. Source/sink interactions underpin crop yield: The case for trehalose 6-phosphate/SnRK1 in improvement of wheat. *Frontiers in Plant Science* **5**: 418.

Leegood RC. **2002**. C_4 photosynthesis: principles of CO_2 concentration and prospects for its introduction into C_3 plants. *Journal of Experimental Botany* **53**: 581–590.

Li P, Ponnala L, Gandotra N, *et al.* 2010. The developmental dynamics of the maize leaf transcriptome. *Nature Genetics* **42**: 1060–1067.

Lovell JT, Jenkins J, Lowry DB, *et al.* 2018. The genomic landscape of molecular responses to natural drought stress in *Panicum hallii*. *Nature Communications 2018 9:1* **9**: 1–10.

Lu CA, Lin CC, Lee KW, *et al.* 2007. The SnRK1A protein kinase plays a key role in sugar signaling during germination and seedling growth of rice. *The Plant Cell* **19**: 2484–2499.

Ludwig M. **2016**. Evolution of carbonic anhydrase in C_4 plants. *Current Opinion in Plant Biology* **31**: 16–22.

Lumbreras V, Albà MM, Kleinow T, Koncz C, Pagès M. **2001**. Domain fusion between SNF1-related kinase subunits during plant evolution. *EMBO Reports* **2**: 55–60.

Lunn JE. **2007**. Compartmentation in plant metabolism. *Journal of Experimental Botany* **58**: 35–47.

Lunn JE, Delorge I, Figueroa CM, Dijck P Van, Stitt M. **2014**. Trehalose metabolism in plants. *The Plant Journal* **79**: 544–567.

Lunn JE, Feil R, Hendriks JHM, *et al.* 2006. Sugar-induced increases in trehalose 6-phosphate are correlated with redox activation of ADPglucose pyrophosphorylase and higher rates of starch synthesis in *Arabidopsis thaliana*. *Biochemical Journal* **397**: 139.

Lunn JE, Furbank RT. **1997**. Localization of sucrose-phosphate synthase and starch in leaves of C_4 plants. *Planta* **202**: 106–111.

Lunn AJE, Furbank RT. **1999**. Tansley Review No . 105 Sucrose biosynthesis in C_4 plants. *JSTOR* **143**: 221–237.

Mallen-Ponce MJ, Perez-Perez ME, Crespo JL. **2022**. Photosynthetic assimilation of CO_2 regulates TOR activity. *Proceedings of the National Academy of Sciences of the United States of America* **119**.

Marshall JS, Stubbs JD, Taylor WC. **1996**. Two genes encode highly similar chloroplastic NADP-Malic enzymes in Flaveria (implications for the evolution of C_4 photosynthesis). *Plant Physiology* **111**: 1251–1261.

Martínez-Barajas E, Delatte T, Schluepmann H, *et al.* 2011. Wheat grain development is characterized by remarkable trehalose 6-phosphate accumulation pregrain filling: Tissue distribution and relationship to SNF1-related protein kinase1 activity. *Plant Physiology* **156**: 373–381.

McCormick RF, Truong SK, Sreedasyam A, *et al.* 2018. The *Sorghum bicolor* reference genome: improved assembly, gene annotations, a transcriptome atlas, and signatures of genome organization. *The Plant Journal* **93**: 338–354.

Mckown AD, Dengler NG. **2007**. Key innovations in the evolution of Kranz anatomy and C_4 vein pattern in Flaveria (Asteraceae). *American Journal of Botany* **94**: 382–389.

Monson RK. **1999**. The origins of C_4 genes and evolutionary pattern in the C_4 metabolic phenotype In: Sage RF, Monson RK, eds. *C4 Plant Biology*. San Diego: Academic Press, 377–410.

Monson RK. **2003**. Gene duplication, neofunctionalization, and the evolution of C_4 photosynthesis. *International Journal of Plant Sciences* **164**: S43–S54.

Moore B, Zhou L, Rolland F, *et al.* 2003. Role of the Arabidopsis glucose sensor HXK1 in nutrient, light, and hormonal signaling. *Science* **300**: 332–336.

Muhaidat R, Sage RF, Dengler NG. **2007**. Diversity of Kranz anatomy and biochemistry in C_4 eudicots. *American Journal of Botany* **94**: 362–381.

Oszvald M, Primavesi LF, Griffiths CA, *et al.* 2018. Trehalose 6-phosphate regulates photosynthesis and assimilate partitioning in reproductive tissue. *Plant Physiology* **176**:

2623–2638.

Ouyang S, Zhu W, Hamilton J, *et al.* 2007. The TIGR Rice Genome Annotation Resource: Improvements and new features. *Nucleic Acids Research* **35**: D883–D887.

Pacheco JM, Canal MV, Pereyra CM, Welchen E, Martínez-Noël GMA, Estevez JM. **2021**. The tip of the iceberg: emerging roles of TORC1, and its regulatory functions in plant cells. *Journal of Experimental Botany* **72**: 4085–4101.

Patro R, Duggal G, Love MI, Irizarry RA, Kingsford C. **2017**. Salmon provides fast and bias-aware quantification of transcript expression. *Nature Methods* **14**: 417–419.

Paul MJ, Watson A, Griffiths CA. **2020**. Trehalose 6-phosphate signalling and impact on crop yield. *Biochemical Society Transactions* **48**: 2127–2137.

Polge C, Jossier M, Crozet P, Gissot L, Thomas M. **2008**. β-subunits of the SnRK1 complexes share a common ancestral function together with expression and function specificities; physical interaction with nitrate reductase specifically occurs via AKINβ1-subunit. *Plant Physiology* **148**: 1570–1582.

Ponnu J, Wahl V, Schmid M. **2011**. Trehalose-6-phosphate: Connecting plant metabolism and development. *Frontiers in Plant Science* **0**: 70.

Rolland F, Baena-Gonzalez E, Sheen J. **2006**. Sugar sensing and signaling in plants: Conserved and novel mechanisms. *Annual Review of Plant Biology* **57**: 675–709.

Rosche E, Westhoff P. **1995**. Genomic structure and expression of the pyruvate, orthophosphate dikinase gene of the dicotyledonous C_4 plant *Flaveria trinervia* (Asteraceae). *Plant Molecular Biology* **29**: 663–678.

Sage RF. **2004**. The evolution of C_4 photosynthesis. *New Phytologist* **161**: 341–370.

Sage RF. **2017**. A portrait of the C_4 photosynthetic family on the 50th anniversary of its discovery: species number, evolutionary lineages, and Hall of Fame. *Journal of Experimental Botany* **68**: e11–e28.

Sage RF, Christin PA, Edwards EJ. **2011**. The C_4 plant lineages of planet Earth. *Journal of Experimental Botany* **62**: 3155–3169.

Schluepmann H, Pellny T, Dijken A van, Smeekens S, Paul M. **2003**. Trehalose 6-phosphate is indispensable for carbohydrate utilization and growth in *Arabidopsis thaliana*. *Proceedings of the National Academy of Sciences* **100**: 6849–6854.

Sekhon RS, Lin H, Childs KL, *et al.* 2011. Genome-wide atlas of transcription during maize development. *The Plant Journal* **66**: 553–563.

Sheen J. **1990**. Metabolic repression of transcription in higher plants. *The Plant cell* **2**: 1027–1038.

Sibout R, Proost S, Hansen BO, *et al.* 2017. Expression atlas and comparative coexpression network analyses reveal important genes involved in the formation of lignified cell wall in *Brachypodium distachyon*. *New Phytologist* **215**: 1009–1025.

da Silva VCH, Martins MCM, Calderan-Rodrigues MJ, *et al.* 2021. Shedding light on the dynamic role of the "Target of Rapamycin" kinase in the fast-growing C_4 species *Setaria viridis*, a suitable model for biomass crops. *Frontiers in Plant Science* **12**: 492.

Stamatakis A. **2006**. RAxML-VI-HPC: maximum likelihood-based phylogenetic analyses with thousands of taxa and mixed models. *Bioinformatics* **22**: 2688–2690.

Stamatakis A. **2014**. RAxML version 8: a tool for phylogenetic analysis and post-analysis of large phylogenies. *Bioinformatics* **30**: 1312–1313.

Tanz SK, Tetu SG, Vella NGF, Ludwig M. **2009**. Loss of the transit peptide and an increase

in gene expression of an ancestral chloroplastic carbonic anhydrase were instrumental in the evolution of the cytosolic C_4 carbonic anhydrase in Flaveria. *Plant Physiology* **150**: 1515–1529.

Tetu SG, Tanz SK, Vella N, Burnell JN, Ludwig M. **2007**. The *Flaveria bidentis* β-carbonic anhydrase gene family encodes cytosolic and chloroplastic isoforms demonstrating distinct organ-specific expression patterns. *Plant Physiology* **144**: 1316–1327.

Tiessen A, Prescha K, Branscheid A, *et al.* 2003. Evidence that SNF1-related kinase and hexokinase are involved in separate sugar-signalling pathways modulating post-translational redox activation of ADP-glucose pyrophosphorylase in potato tubers. *The Plant Journal* **35**: 490–500.

Turgeon R, Webb JA. **1976**. Leaf development and phloem transport in *Cucurbita pepo*: Maturation of the minor veins. *Planta* **129**: 265–269.

Vogel JP, Garvin DF, Mockler TC, *et al.* 2010. Genome sequencing and analysis of the model grass *Brachypodium distachyon*. *Nature* **463**: 763–768.

Wang L, Czedik-Eysenberg A, Mertz RA, *et al.* 2014. Comparative analyses of C_4 and C_3 photosynthesis in developing leaves of maize and rice. *Nature Biotechnology* **32**: 1158–1165.

Washburn JD, Strable J, Dickinson P, *et al.* 2021. Distinct C_4 sub-types and C_3 bundle sheath isolation in the Paniceae grasses. *Plant Direct* **5**: e373.

Watson-Lazowski A, Papanicolaou A, Sharwood R, Ghannoum O. **2018**. Investigating the NAD-ME biochemical pathway within C_4 grasses using transcript and amino acid variation in C_4 photosynthetic genes. *Photosynthesis Research* **138**: 233–248.

Westhoff P, Gowik U. **2010**. Evolution of C_4 Photosynthesis—Looking for the Master Switch. *Plant Physiology* **154**: 598–601.

Whitney SM, Sharwood RE, Orr D, White SJ, Alonso H, Galmés J. **2011**. Isoleucine 309 acts as a C_4 catalytic switch that increases ribulose-1,5-bisphosphate carboxylase/oxygenase (Rubisco) carboxylation rate in Flaveria. *Proceedings of the National Academy of Sciences of the United States of America* **108**: 14688–14693.

Wingler A, Fritzius T, Wiemken A, Boller T, Aeschbacher RA. **2000**. Trehalose induces the ADP-glucose pyrophosphorylase gene, *ApL3*, and starch synthesis in Arabidopsis. *Plant Physiology* **124**: 105–114.

Xiong Y, McCormack M, Li L, Hall Q, Xiang C, Sheen J. **2013**. Glucose–TOR signalling reprograms the transcriptome and activates meristems. *Nature* **496**: 181–186.

Xiong Y, Sheen J. **2012**. Rapamycin and glucose-target of rapamycin (TOR) protein signaling in plants. *Journal of Biological Chemistry* **287**: 2836–2842.

Xiong Y, Sheen J. **2014**. The role of Target of Rapamycin signaling networks in plant growth and metabolism. *Plant Physiology* **164**: 499–512.

Xu B, Yang Z. **2013**. pamlX: A Graphical User Interface for PAML. *Molecular Biology and Evolution* **30**: 2723–2724.

Yue H, Wang L, Liu H, *et al.* 2016. *De novo* assembly and characterization of the transcriptome of Broomcorn Millet (*Panicum miliaceum* L.) for gene discovery and marker development. *Frontiers in Plant Science* **7**.

Zhang G, Liu X, Quan Z, *et al.* 2012. Genome sequence of foxtail millet (*Setaria italica*) provides insights into grass evolution and biofuel potential. *Nature Biotechnology* **30**: 549–554.

Zhang J, Nielsen R, Yang Z. **2005**. Evaluation of an improved branch-site likelihood method for detecting positive selection at the molecular level. *Molecular Biology and Evolution* **22**:

2472–2479.

Zhang Y, Primavesi LF, Jhurreea D, *et al.* 2009. Inhibition of SNF1-Related Protein Kinase1 activity and regulation of metabolic pathways by Trehalose-6-Phosphate. *Plant Physiology* **149**: 1860–1871.

Zhang Y, Shewry PR, Jones H, Barcelo P, Lazzeri PA, Halford NG. **2001**. Expression of antisense SnRK1 protein kinase sequence causes abnormal pollen development and male sterility in transgenic barley. *The Plant Journal* **28**: 431–441.

Zhang J, Zhang X, Tang H, *et al.* 2018. Allele-defined genome of the autopolyploid sugarcane *Saccharum spontaneum* L. *Nature Genetics* **50**: 1565–1573.

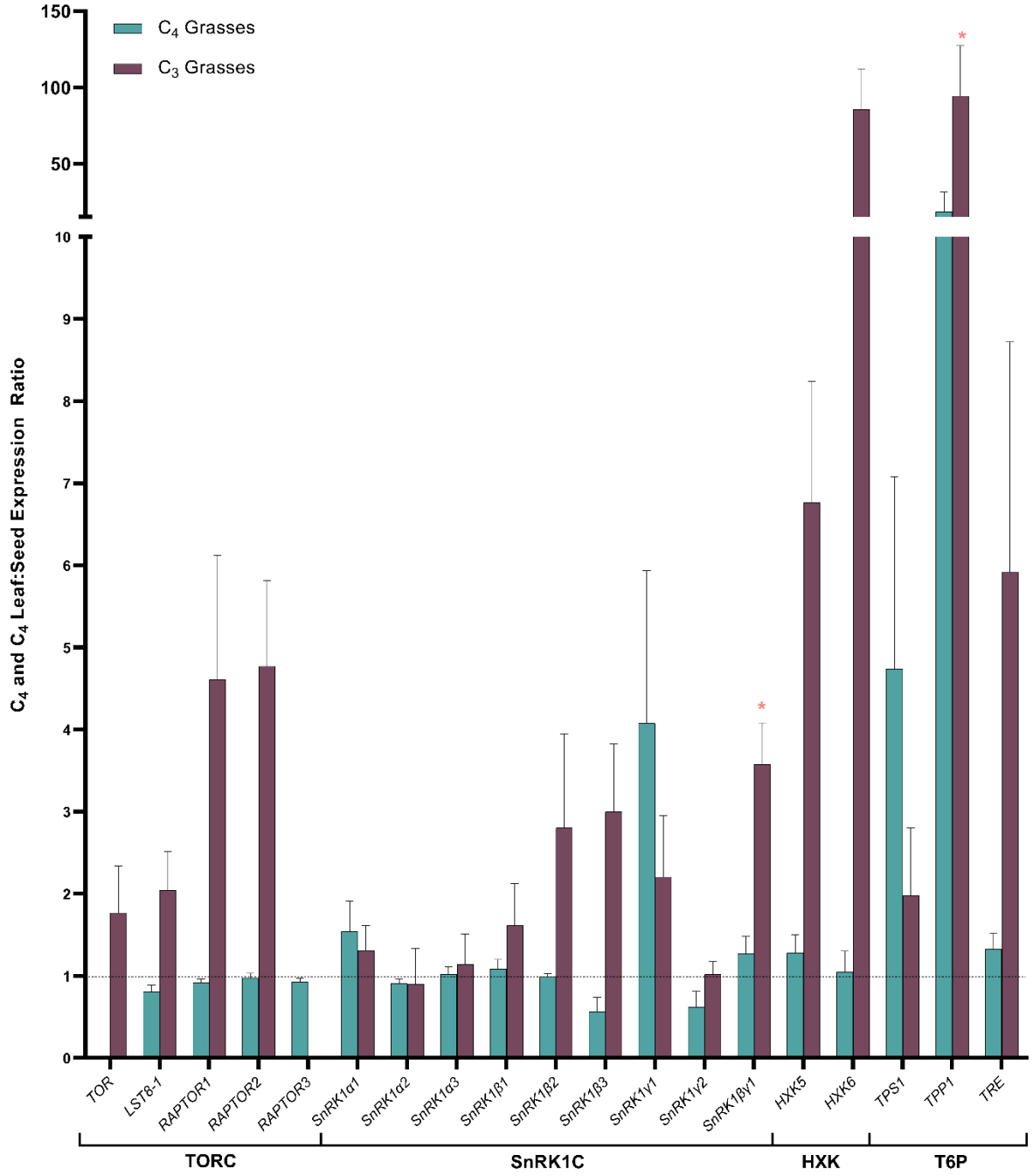

Fig. 1 Leaf to seed expression ratio of sugar sensor gene comparisons between C_4 and C_3 grasses.

RMA-normalised or TPM values from either microarray or RNAseq data of sugar sensor genes were used to calculate leaf to seed ratios from the C_4 grasses *Zea mays* and *Panicum miliaceum* and the C_3 grasses *Oryza sativa* and *Brachypodium distachyon* (Jain *et al.* 2007; Sekhon *et al.* 2011; Yue *et al.* 2016; Sibout *et al.* 2017). Each species consisted of three biological replicates for each tissue sampled. Data represents the mean leaf to seed ratios of genes from C_4 and C_3 grasses (n=6). Error bars represent the SEM. Ratios <1 indicate expression of the gene predominating in the seed whereas >1 indicate expression predominating in the leaf. Broken

line indicates 1. Red asterisks represent significant difference to 1 and predominating in the leaf. There were no genes expressed with a ratio <1 that were significantly different.

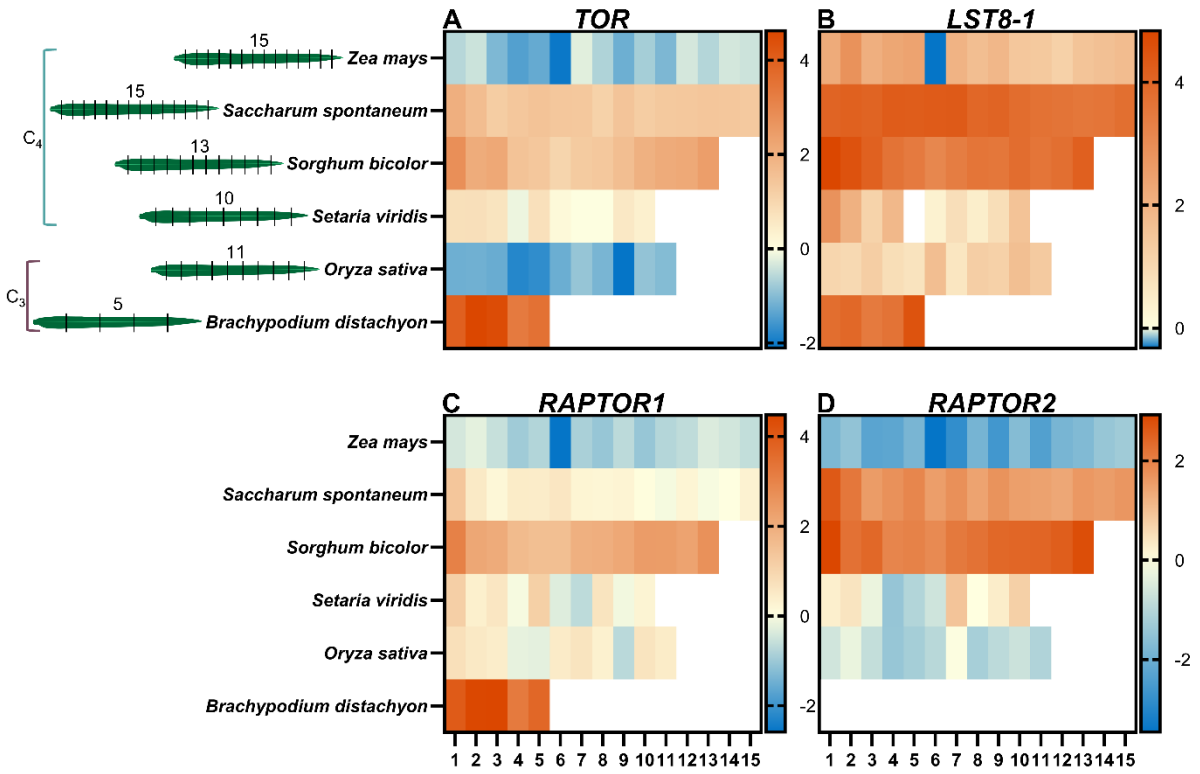

Fig. 2 Expression of genes encoding TORC subunits along the leaf gradient of C_4 and C_3 grasses.

Heat maps displaying $\log_2$ TPM values of the genes *TOR* (A), *LST8-1* (B), *RAPTOR1* (C), *RAPTOR2* (D) encoding subunits that make up TORC. *RAPTOR3* was omitted due to its absence in multiple genomes. *RAPTOR2* was absent in the Brachypodium genome. The C_4 species examined were *Zea mays* (15 sections), *Saccharum spontaneum* (15 sections), *Sorghum bicolor* (13 sections) and *Setaria viridis* (10 sections), with the C_3 species being *Oryza sativa* (11 sections) and *Brachypodium distachyon* (5 sections) (Li *et al.* 2010; Wang *et al.* 2014; Ding *et al.* 2015; Hu *et al.* 2018). Leaf sectioning is indicated to the left (A). Where expression within a leaf section is represented as white indicated no detectable reads. Scale bar to the right of each heatmap represent $\log_2$ TPM.

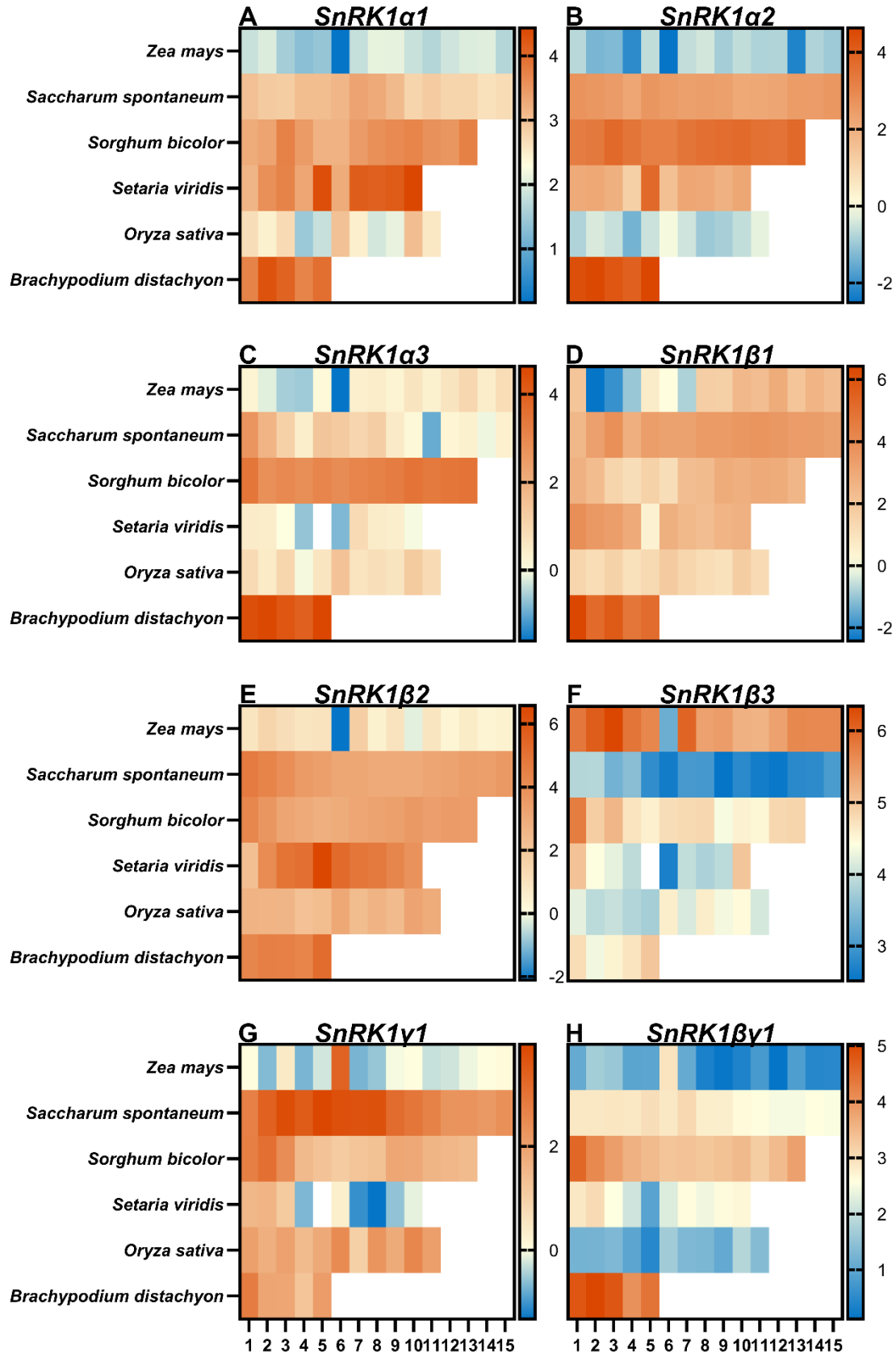

Fig. 3 Expression of genes encoding SnRK1C subunits along the leaf gradient of C_4 and C_3 grasses.

Heat maps displaying log_2 TPM values of the genes *SnRK1α1* (A), *SnRK1α2* (B), *SnRK1α3* (C), *SnRK1β1* (D), *SnRK1β2* (E), *SnRK1β3* (F), *SnRK1γ1* (G), SnRK1βγ1 (H) encoding subunits that make up SnRK1C. *SnRK1γ2* and *SnRK1βγ2* were omitted due their absence in the genome or low to no expression within the species. The C_4 species examined were *Zea mays* (15 sections), *Saccharum spontaneum* (15 sections), *Sorghum bicolor* (13 sections) and *Setaria viridis* (10 sections), with the C_3 species being *Oryza sativa* (11 sections) and *Brachypodium distachyon* (5 sections) (Li *et al.* 2010; Wang *et al.* 2014; Ding *et al.* 2015; Hu *et al.* 2018). Where expression within a leaf section is represented as white indicated no detectable reads. Scale bar to the right of each heatmap represent log_2 TPM.

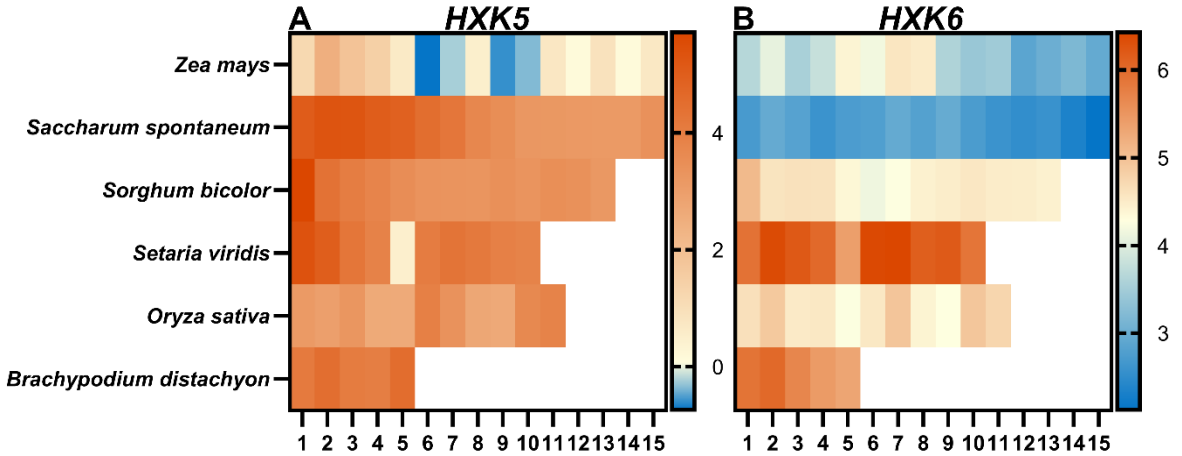

Fig. 4 Expression of genes encoding putative sugar sensing hexokinases along the leaf gradient of C_4 and C_3 grasses.

Heat maps displaying log_2 TPM values of the genes *HXK5* (A), *HXK6* (B). The C_4 species examined were *Zea mays* (15 sections), *Saccharum spontaneum* (15 sections), *Sorghum bicolor* (13 sections) and *Setaria viridis* (10 sections), with the C_3 species being *Oryza sativa* (11 sections) and *Brachypodium distachyon* (5 sections) (Li *et al.* 2010; Wang *et al.* 2014; Ding *et al.* 2015; Hu *et al.* 2018). Scale bar to the right of each heatmap represent log_2 TPM.

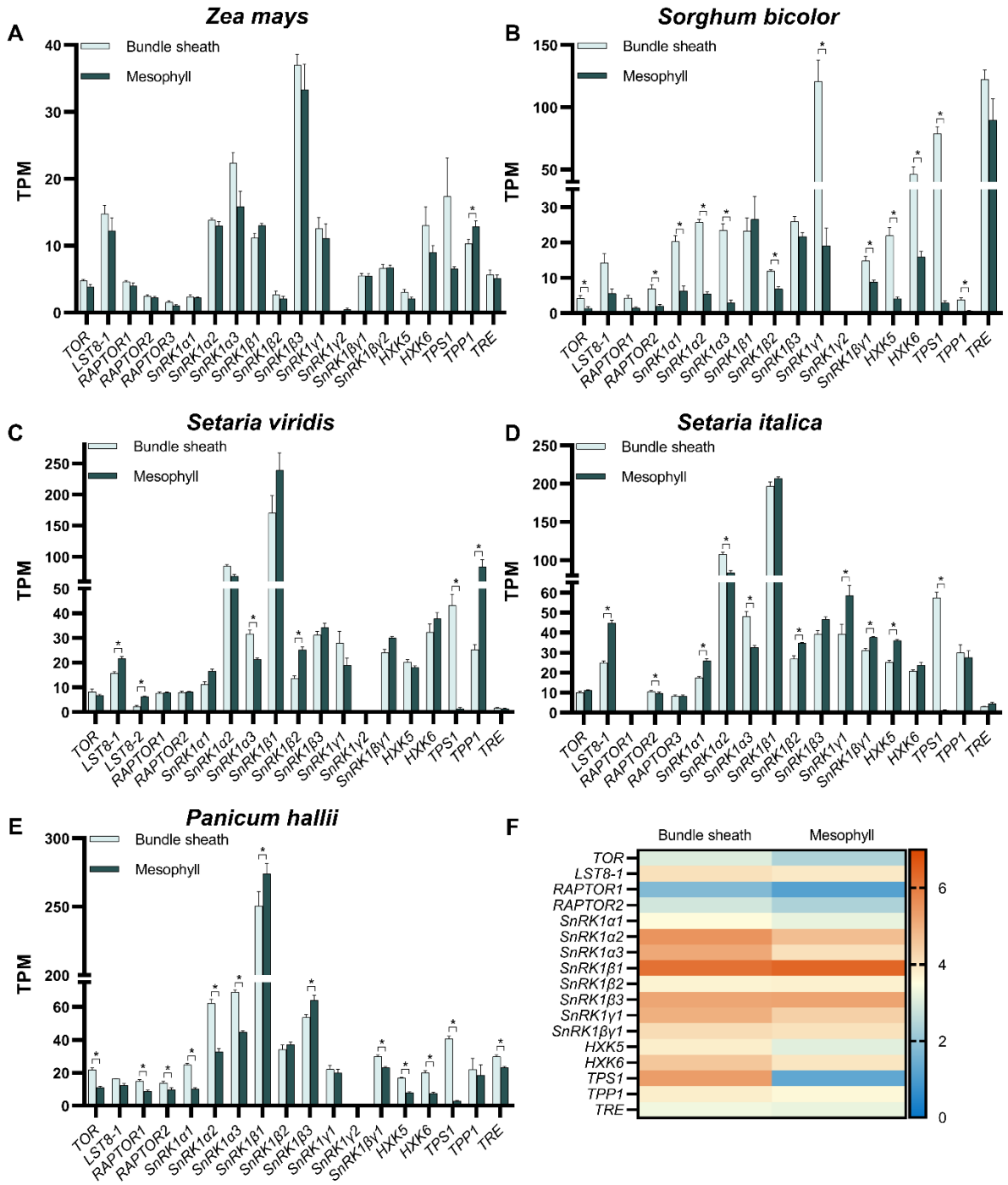

Fig. 5 Expression of genes encoding proteins involved in T6P signalling along the leaf gradient of C_4 and C_3 grasses.

Heat maps displaying $\log_2$ TPM values of the genes *TPS1* (A), *TPP* (B), *TRE* (C). The C_4 species examined were *Zea mays* (15 sections), *Saccharum spontaneum* (15 sections), *Sorghum bicolor* (13 sections) and *Setaria viridis* (10 sections), with the C_3 species being *Oryza sativa* (11 sections) and *Brachypodium distachyon* (5 sections) (Li *et al.* 2010; Wang *et al.* 2014; Ding *et al.* 2015; Hu *et al.* 2018). Where expression within a leaf section is represented as white indicated no detectable reads. Scale bar to the right of each heatmap represent $\log_2$ TPM.

Fig. 6 Sugar sensor gene expression between bundle sheath and mesophyll cells of C_4 grasses. *Zea mays* (A). *Sorghum bicolor* (B). *Setaria viridis* (C). *Setaria italica* (D). *Panicum hallii* (E) (John *et al.* 2014; Döring *et al.* 2016; Denton *et al.* 2017; Washburn *et al.* 2021). Heatmap comparison of $\log_2$ TPM means of bundle sheath and mesophyll expression in C_4 grasses (F). A student's t-test was performed between the bundle sheath and mesophyll cell expression of each gene from each species ($P<0.05$). Asterisk denotes significantly different expression between bundle sheath and mesophyll cells.

Table 1 Sugar sensor genes present in C_4 and C_3 grasses. *Brachypodium distachyon* (Bd), *Oryza sativa* (Os), *Panicum hallii* (Ph), *Panicum miliaceum* (Pm) *Sorghum bicolor* (Sb), *Setaria italica* (Si), *Setaria viridis* (Sv), *Saccharum spontaneum* (Ss), and *Zea mays* (Zm). "X" denotes the presence of the gene within the genome of the corresponding species.

Gene	Bd	Os	Zm	Pm	Sv	Ss	Sb	Si	Ph
TOR	X	X	X	X	X	X	X	X	X
LST8-1	X	X	X	X	X	X	X	X	X
RAPTOR1	X	X	X	X	X	X	X	X	X
RAPTOR2		X	X	X	X	X	X	X	X
RAPTOR3	X		X	X		X		X	
SnRK1α1	X	X	X	X	X	X	X	X	X
SnRK1α2	X	X	X	X	X	X	X	X	X
SnRK1α3	X	X	X	X	X	X	X	X	X
SnRK1β1	X	X	X	X	X	X	X	X	X
SnRK1β2	X	X	X	X	X	X	X	X	X
SnRK1β3	X	X	X	X	X	X	X	X	X
SnRK1γ1	X	X	X	X	X	X	X	X	X
SnRK1γ2	X	X	X	X	X	X	X	X	X
SnRK1βγ1	X	X	X	X	X	X	X	X	X
SnRK1βγ2			X	X		X			
HXK1		X							
HXK2	X	X							
HXK3	X	X	X	X	X	X	X	X	X
HXK5	X	X	X	X	X	X	X	X	X
HXK6	X	X	X	X	X	X	X	X	X
HXK4	X	X	X						
HXK7	X	X	X		X	X	X	X	X
HXK8	X		X	X	X	X	X	X	X
HXK9	X	X	X	X		X	X		
HXK10	X	X	X	X	X	X	X	X	X
TPS1	X	X	X	X	X	X	X	X	X
TPP1	X	X	X	X	X	X	X	X	X
TRE	X	X	X	X	X	X	X	X	X